AD

AD-E401 140

TECHNICAL REPORT ARLCD-TR-84002

SHOCK FRONT PUMPED STOKES AND ANTI-STOKES REFLECTIVITY CONTRIBUTIONS

PAUL HARRIS
ARDC

HENRI-NÖEL PRESLES
UNIVERSITY POITIERS, FRANCE

MARCH 1984

U.S. ARMY ARMAMENT RESEARCH AND DEVELOPMENT CENTER
LARGE CALIBER WEAPON SYSTEMS LABORATORY
DOVER, NEW JERSEY

ACKNOWLEDGMENTS

The authors are indebted to Y. Sarazin and H. Simonnet (both of the University de Poitiers) for experimental assistance, and to R. Alfano and his group (at the Ultrafast Spectroscopy Laboratory, City College of New York) for helpful discussions concerning spectroscopic effects.

CONTENTS

FIGURES

INTRODUCTION

Reflectivity is associated with an interface between media of different refractive indices. The front of a mass density shock wave causes a change in refractive index by forcing a change in the spatial density or character of the optical scattering sites and/or the magnitude of electric moment-field interaction matrix elements. It has thus been clear for some time that employing a propagating shock front as a reflectivity surface permits the study of details of the transition between the shocked and the unshocked states, as well as the possibility of understanding the molecular level contributions to the index of refraction.

Until now shock front reflectivity experiments have been used primarily as a tool for estimating the thickness of the shock transition region (refs 1 to 3), with the classic work being that of Cowan and Hornig (shock front thickness in gases) (ref 1). More recently, however, we have attempted a very detailed comparison between theoretical and experimental reflectivities for shocked liquid water at 5.8 kbar (0.58 GPa) and have found a difference between theory and experiment which cannot be explained by employing a refined (secondary reflection) Fresnel reflectivity theory (ref 4) (fig. 1).

A large discrepancy exists between the theoretically predicted and experimental reflectivities for the parallel-to-the-plane-of-incidence optical polarization, as illustrated in figure 1. That discrepancy increases as the optical angle of incidence increases or, equivalently, as the direction of the $\tilde{E}$ field of the reflecting beam becomes more and more parallel to the direction of shock propagation (see insert fig. 1). Because the case of the perpendicular-to-the-plane-of-incidence polarization yields quite good agreement between theory and experiment, the parallel-to-the-plane-of-incidence dependence on angle strongly suggests that the shock front must be strongly influencing those terms in the optical scattering matrix which have an initial and/or final electric dipole moment state in the direction of shock propagation.

An analogous case exists where a low power laser probe beam is used to sample a material which has had optical phonon states pumped with a preferred directionality by the imposition of a high powered laser beam (stimulated Raman scattering) (ref 5). In that case, the interaction of the probe beam and the optical phonon diminishes the probe beam intensity and creates side band beams (Stokes and anti-Stokes) which are spatially separated from the probe beam.

This report demonstrates that the one-dimensional strain shock front region (the transition region between two differing mass density hydrostatic states of water) could serve as a mechanical pump in the creation of excited (i.e., otherwise relatively unpopulated) electric dipole states in the liquid water. The reflectivity measuring laser beam then would become equivalent to the above-mentioned probe beam, and that reflectivity beam would interact with the excited states of the shock front region forming side bands. This would clearly have an effect upon the measured reflectivity. For example, the finite angular width of the photo diode means that the non-interacted part of the reflectivity beam and a spatially separated side band are not simultaneously imaged on the photo diode.

SHOCK FRONT PUMPED EXCITED STATES

The probe beam, excited state, and side band geometry shown in figure 2 assumes that the excited state wave vector, $\underset{\sim}{k}_\nu$, is parallel to the direction of shock propagation. For probe (reflectivity) beam frequency ω and excited state energy $\hbar\omega_\nu$, the conservation of momentum and energy leads to

$$\underset{\sim}{k}' = \underset{\sim}{k} + \underset{\sim}{k}_\nu \tag{1}$$

$$\frac{k'}{k} = 1 + \frac{\omega_\nu}{\omega} \tag{2}$$

If the z (shock propagation direction) component of equation 1 is combined with equation 2 and

$$k_z' = k' \cos(\theta - \psi) \tag{3}$$

then

$$\frac{k_\nu}{k} = \left(1 + \frac{\omega_\nu}{\omega}\right) \cos(\theta - \psi) - \cos\theta \tag{4}$$

so that knowledge of θ, ψ, and $\left(\frac{\omega_\nu}{\omega}\right)$ yields a value for k_ν.

By manipulating equations 1, 2, and 3, it can be shown that

$$\begin{aligned}\sin^2\theta = &- \left(1 + \frac{\omega_\nu}{\omega}\right)^2 \sin^2\theta \cos^2\psi + \\ &+ 2\left(1 + \frac{\omega_\nu}{\omega}\right)^2 \sin\theta \cos\theta \sin\psi \cos\psi + \\ &- \left(1 + \frac{\omega_\nu}{\omega}\right)^2 \sin^2\psi \cos^2\theta + \\ &+ 2\left(1 + \frac{\omega_\nu}{\omega}\right) \sin^2\theta \cos\psi + \\ &- 2\left(1 + \frac{\omega_\nu}{\omega}\right) \sin\theta \cos\theta \sin\psi\end{aligned} \tag{5a}$$

or, to first order in ψ,

$$\begin{aligned}\sin^2\theta = &- \left(1 + \frac{\omega_\nu}{\omega}\right)^2 \sin^2\theta + 2\psi\left(1 + \frac{\omega_\nu}{\omega}\right)^2 \sin\theta \cos\theta + \\ &+ 2\left(1 + \frac{\omega_\nu}{\omega}\right) \sin^2\theta - 2\psi\left(1 + \frac{\omega_\nu}{\omega}\right) \sin\theta \cos\theta\end{aligned} \tag{5b}$$

Equation 5b yields for ψ

$$\psi = \frac{1}{2} \frac{\left(\frac{\omega_\nu}{\omega}\right)}{\left(1 + \frac{\omega_\nu}{\omega}\right)} \tan \theta \qquad (6a)$$

Employing the same approach as above, it is possible to show that, if $\tilde{k}_\nu$ makes an angle ϕ with respect to the direction of shock propagation, then, again to first order in ψ,

$$\psi = \frac{1}{2} \frac{\left(\frac{\omega_\nu}{\omega}\right)}{\left(1 + \frac{\omega_\nu}{\omega}\right)} \left[\frac{\cos^2 \phi - \cos^2 \theta}{\cos \theta \sin \theta}\right] \qquad (6b)$$

Because the difference between $\tan \theta$ and $\left[\frac{\cos^2 \phi - \cos^2 \theta}{\cos \theta \sin \theta}\right]$ is small for θ approximately 75 degrees and ϕ approximately 10 degrees, only ψ given by equation 6a will be considered in the following analyses (i.e., $\phi = 0$ is assumed).

Equation 6a and figure 3 show that $\omega_\nu > 0$ (corresponding to anti-Stokes radiation) gives $\psi_{AS} > 0$ and represents the earliest signal to be imaged on the photo-diode. $\omega_\nu < 0$ (corresponding to Stokes radiation) gives $\psi_S < 0$ and represents the last signal (as the shock front sweeps down the sample) to be imaged on the photo-diode.

The essential idea is that within the shock front region, optically active excited states separated by energy $h\omega_\nu$ are caused to exist and transitions between those states make up reflectivity side bands when the momentum conserving $\tilde{k}_\nu$ states are available. Normally such side band signals are observed spectroscopically by studying optical intensity as a function of frequency. In the case of the measurements of the shock front optical reflectivity discussed here, however, it is the spatial separation associated with the side band signals that is potentially observed.

A typical parallel-to-the-plane-of-incidence (optical polarization) noise averaged photo-diode record is illustrated in figure 4. If $(t_C - t_B)$ is taken as the separation between the main reflection signal and the anti-Stokes signal at the converging lens photo-diode system, then

$$(t_C - t_B) = \frac{\psi R \sin \theta}{U_S} \qquad (7)$$

where U_S is the shock velocity, and R is the distance from the scattering volume to the converging lens photo diode system. Equation 7 assumes scattering volume dimensions are small compared to R (which was satisfied experimentally), and that the beam diameter is less than beam-side band separation at the photo-diode. The laser beam always had a diameter of approximately 0.3 mm at the scattering volume (prior to scattering). It is assumed that the main (scattered) reflectivity beam was less than 1 mm in diameter at the photo-diode.

For the typical experimental values of R = 23 cm, $U_S \sim 2.1 \times 10^5$ cm/sec at 5.8 kbar (ref 6), $(t_C - t_B) \sim 0.8$ μ sec, and optical angle of incidence of 78 degrees

$$\psi_{AS} \text{ (78 degrees)} \sim 0.43 \text{ degree} \tag{8a}$$

0.27 degree corresponds to ~ 1 mm at 23 cm. Thus, from equation 6a,

$$\frac{\omega_\nu}{\omega} \sim 3.2 \times 10^{-3} \tag{8b}$$

For $\omega = 2\pi f$ and $f = (5145 \text{ Å})^{-1}$ corresponding to the wavelength of the reflectivity laser employed in these experiments, equation 8b gives†

$$f_\nu \sim 61 \text{ cm}^{-1} \tag{8c}$$

Equation 8c substituted into equation 4 yields

$$\frac{k_\nu}{k}\Big|_{AS} \sim 8.0 \times 10^{-3} \tag{8d}$$

If the value for k within the scattering medium (water) is used, then $k = 2\pi n\lambda^{-1}$ with n = 1.33 (the index of refraction) and λ = 5145 Å gives from equation 8d

$$k_\nu \Big|_{AS} \text{ (78 degrees)} \sim 1.3 \times 10^3 \text{ cm}^{-1} \tag{8e}$$

The $f_\nu \sim 61 \text{ cm}^{-1}$ value from equation 8c, which actually is good to only one significant figure, is to be compared with Raman signals observed near 175 cm^{-1} and 60 cm^{-1} by Walrefen in water (ref 7), and near 190 cm^{-1} and 50 cm^{-1} (inferred) infrared signals observed in ice by Bertie and Whalley (ref 8). The ~ near 60 cm^{-1} (50 cm^{-1}) signal has been associated with transverse displacements (bending) of the intermolecular OH bond in tetrahedrally bonded water (refs 7 and 8).

Setting $\left(\frac{\omega_\nu}{\omega}\right) \sim -3.2 \times 10^{-3}$ in equation 8b yields the corresponding Stokes line with a corresponding separation angle (again as a first order quantity) given by

$$\psi_S \text{ (78 degrees)} \sim -0.43 \text{ degree} \tag{9a}$$

---

† Spectroscopic units (i.e., cm^{-1}) are used for frequencies in this report. Ordinary frequency units are obtained by multiplying the spectroscopic units by the speed of light.

with the corresponding result

$$\frac{k_\nu}{k}\Big|_S \sim -\ 8.0 \times 10^{-3} \tag{9b}$$

and

$$k_\nu\Big|_S \sim -\ 1.3 \times 10^{3}\ \text{cm}^{-1} \tag{9c}$$

The minus sign in equation 9c indicates that the phonon state responsible for conserving momentum in the Stokes process is an emitted phonon which is directed opposite to the direction of shock propagation. Remembered that only k_ν states parallel to the direction of shock propagation are considered here ($\phi = 0$ in equation 6b has been assumed).

DISCUSSION

The number of phonon states contributing to the Stokes and anti-Stokes signals can be estimated from the known reflectivity coefficient (~ 5% at 78 degree angle of incidence) for the 1-watt CW laser beam which is scattered into the lens-photo-diode system for approximatley 2 μ sec. If it is assumed that the Stokes and anti-Stokes signals have intensities approximately equal to the simple reflectivity (which appears to be the experimental situation at 5.8 kbar and 78 degree angle-of-incidence) then, since approximately 1 erg of the laser beam is converted into Stokes or anti-Stokes radiation,

$N_p \equiv$ number of side band photons

$$N_p \sim \frac{1\ \text{erg}}{\hbar\omega} \sim 3 \times 10^{11}\ \text{photons} \tag{10}$$

The comparison of the N_p value with the expected room temperature thermal equilibrium phonon occupation for ω_ν (k_ν) states is interesting. Whether the expression

$$N_\nu^{(1)}(T) \equiv \frac{L}{2\pi}\left\{\exp\left(\frac{\hbar\omega_\nu}{kT}\right) - 1\right\}^{-1} dk_\nu \tag{11a}$$

is employed for one-dimensional physics or

$$N_\nu^{(3)}(T) \equiv \frac{V}{(2\pi)^3}\left\{\exp\left(\frac{\hbar\omega_\nu}{kT}\right) - 1\right\}^{-1} k_\nu^2\, d\, k_\nu \tag{11b}$$

for three-dimensional physics, with $dk_\nu \sim k_\nu$, and whether $V = 1\ cm^3$, $L = 1$ cm or expected (ref 9) shock front thickness and laser beam cross section related values ($V = 2 \times 10^{-9}\ cm^3$, $L = 20$ Å) the result is $N_\nu(T) << N_p$ by at least six orders of magnitude.

Such large differences between $N_\nu(T)$ and N_p have already been observed (ref 10) for laser pumped stimulated Raman spectroscopy (SRS) experiments and implied in theoretical considerations by Coffey and Toton (ref 11).

The implication of the difference between $N_\nu(T)$ and N_p is clear. The shock front region pumps up phonon states to occupancies far greater than either the thermal equilibrium state before the shock front or the thermal equilibrium state after the shock front. The shock front region should thus be viewed as physically different, in the strongest sense possible, from the overall entity known as a shock wave. This, if correct, represents a first for mass-density shock wave physics: the availability of an experimental tool capable of observing the states within the shock front region in detail.

Any study which claims that mass density shock pumped Raman spectroscopic effects are making a contribution to shock front reflectivity measurements must attempt to calculate the intensities of the Raman lines. It is relatively easy to show that any intensity calculation based on equilibrium effects, such as that contained in the Rayleigh ratio value $R_{90^0,u} \sim 10^{-6}\ cm^{-1}$ for water (ref 12) will give intensities at the photo-detection system approximately six orders-of-magnitude smaller than are required to explain observations. That is not surprising in light of the previous comments concerning the difference in phonon occupation within the shock front region as compared to the equilibrium state. Fortunately, it is possible to carry out a simple calculation for the Raman scattered field strength based upon a simply stated nonequilibrium contribution.

The scattered field strength, $\underset{\sim}{E}'$, at the detection system may be shown (ref 13) to satisfy the relation

$$\overline{|\underset{\sim}{E}'|^2} = \frac{\pi^2 \overline{|\underset{\sim}{G}|^2} \sin^2 \psi}{R_o^2 \varepsilon^2 \lambda^4} \tag{12}$$

where

$$\overline{|\underset{\sim}{G}|^2} = E_{oi} E_{ok}^* \int \delta\varepsilon_{\ell i}\, dV \int \delta\varepsilon_{\ell k}\, dV \tag{13}$$

R_o is the distance between the photo-detection system and the scattering volume, ε is the scalar dielectric constant, ψ is as employed in figure 2, $\underset{\sim}{E}_o$ is the incident field strength, $\delta\varepsilon_{\ell i}$ is the instantaneous amplitude of the fluctuation of the permittivity, dV is a differential element of the scattering volume, and the bar indicates an average over the molecular motion.

Let us approximate the contents of equation 13 by

$$G_i = (\delta\varepsilon_{ij}) E_{oj} V_{scatt} \tag{14}$$

and, appropriate to a one-dimensional (strain) shock problem,

$$\delta\varepsilon_{ij} \equiv (\delta\varepsilon)\ \delta_{i1}\ \delta_{j1} \tag{15}$$

where the delta function subscript 1 indicates the direction of shock propagation. Clearly equation 15, when applied to the perpendicular-to-the-plane-of-incidence optical polarization case, yields $\underset{\sim}{G}_{\perp} = 0$. The parallel-to-plane-of-incidence case, where $\underset{\sim}{E}_o$ is perpendicular to $\underset{\sim}{k}$ and in the plane formed by $\underset{\sim}{k}$ and $\underset{\sim}{k}'$, yields

$$\vec{G}_{11} = \hat{\varepsilon}_1\ (\delta\varepsilon)\ E_o\ V_{scatt}\ \sin\theta \tag{16}$$

where $\hat{\varepsilon}_1$ is a unit vector in the direction of shock propagation and θ is the angle of optical incidence.

If ℓ is the laser beam diameter, then consideration of the projection of the beam diameter on the shock front within the plane of incidence gives

$$V_{scatt} = \frac{L\,\ell^2}{\cos\theta} \tag{17}$$

where is the shock front thickness. Combining equations 12, 16, and 17 results in

$$\left|\frac{E'}{E_o}\right|^2 = \frac{\pi^2 L^2 \ell^4}{\lambda^4 R_o^2} \overline{\left(\frac{\delta\varepsilon}{\varepsilon}\right)^2} \tan^2\theta \sin^2\psi \tag{18}$$

Substituting from equation 6a then gives

$$\left|\frac{E'}{E_o}\right|^2 = \frac{\pi^2 L^2 \ell^4}{4\lambda^4 R_o^2} \overline{\left(\frac{\delta\varepsilon}{\varepsilon}\right)^2} \left(\frac{\omega_\nu}{\omega}\right)^2 \tan^4\theta \tag{19}$$

where $\omega_\nu << \omega$ has been assumed.

Substituting L = 20 Å, ℓ = 1 mm, $\lambda = 5 \times 10^{-5}$ cm, and R_o = 23 cm into equation 19 yields

$$\left|\frac{E'}{E_o}\right|^2 = 3.0 \times 10^{-3} \overline{\left(\frac{\delta\varepsilon}{\varepsilon}\right)^2} \left(\frac{\omega_\nu}{\omega}\right)^2 \tan^4\theta \tag{20a}$$

If $\overline{\left(\frac{\delta\varepsilon}{\varepsilon}\right)^2} = 1$, representing a strong non-equilibrium shock front induced permittivity fluctuation, is used along with $\left(\frac{\omega_\nu}{\omega}\right) \sim 3.2 \times 10^{-3}$ from equation 8b and θ = 78 degrees the result is

$$\left|\frac{E'}{E_o}\right|^2 \sim 1.5 \times 10^{-5} \qquad (20b)$$

While the reflectivity contribution indicated by equation 20b is approximately three orders-of-magnitude smaller than necessary to explain experimental observations, it is at the same time approximately three orders-of-magnitude larger than a typical equilibrium Rayleigh ratio contribution.

The sin ψ term, with small ψ, in equation 18 is the principal reason for equation 20b being smaller than necessary. There is, however, another Stokes and anti-Stokes contribution which does not suffer from the small ψ effect. To this point we have only considered the Stokes and anti-Stokes contributions relative to (generated by) the simple reflected beam labeled $\underset{\sim}{k}$ in figure 2. It is also possible to have a contribution from the same scattering volume relative to (generated by) the incoming laser beam.

For the one-dimensional permittivity fluctuation of equation 15 it is possible to show that, for an incoming beam $\underset{\sim}{k}$ making an angle θ with respect to the normal to the shock front, equation 18 becomes

$$\left|\frac{E'}{E_o}\right|^2 = \frac{\pi^2 L^2 \ell^2}{\lambda^4 R_o^2} \overline{\left(\frac{\delta\varepsilon}{\varepsilon}\right)^2} \tan^2\theta \sin^2\theta \qquad (21a)$$

where again $\underset{\sim}{E}'$ is non-zero only for the parallel-to-the-plane-of-incidence optical polarization, and $\underset{\sim}{E}'$ itself is entirely within the plane of incidence. Employing the same values for the parameters in equation 21 as were employed with equations 20 gives

$$\left|\frac{E'}{E_o}\right|^2 = 5.3 \times 10^{-2} \qquad (21b)$$

An approximately 5% Stokes and anti-Stokes reflectivity contribution is more than sufficient to explain the larger than expected water reflectivity signals for the parallel to optical plane of incidence case (ref 4).

The effect associated with equation 21a also has the desirable properties of an increasing contribution for an increasing angle of incidence θ, and a zero contribution for $\underset{\sim}{E}_o$ perpendicular to optical plane of incidence. Both properties are in agreement with experimental observation (ref 4).

The geometry associated with equation 15, which is equivalent as a phenomenon to saying that $\underset{\sim}{k}_\nu$ is normal to the shock front, restricts $\underset{\sim}{E}'$ in equations 18 and 21a to be entirely within the plane of incidence. If the equation 15 condition is relaxed, then two effects occur:

1. A parallel-to-the-plane-of-incidence incoming beam will have a Stokes and anti-Stokes reflectivity contribution with perpendicular-to-the-plane-of-incidence components.

2. A perpendicular-to-the-plane-of-incidence incoming beam will have non-zero Stokes and anti-Stokes reflectivity contributions.

The first of these two effects is potentially the most interesting, because such an effect, not predicted to exist for simple reflectivity, represents a decisive experiment which can be simply carried out in a typical shock wave laboratory. For the parallel-to-the-plane-of-incidence reflectivity experiment a polarization analyzer at the photo-detection system must be added. The analyzer would be polarized perpendicular to the incidence so that only Stokes and anti-Stokes contributions would be observable.

For tetrahedral hydrogen bonded water there will be some shock compressed hydrogen bonds at non-zero angle relative to the direction of shock propagation. Thus it is reasonable to expect an out of the optical plane of incidence polarization contribution, although perhaps small in amplitude, if the basic ideas contained within this paper are correct.

CONCLUSIONS

We have postulated Stokes and anti-Stokes contributions to the shock front optical reflectivity. Those contributions, viewed here as arising only from the shock front region, represent a new and important tool for probing the transition between the unshocked and shocked states.

In the near future these authors intend to look for perpendicular-to-the plane-of-incidence signals with a parallel-to-the-plane-of-incidence incoming beam. Also, employing laser-generated shock waves in water at approximately 5 kbar amplitude, the Ultrafast Spectroscopy and Laser Physics Laboratory at the City College of New York will soon search for Raman frequency shifted lines within the shock front reflected signal.

REFERENCES

1. G. R. Cowan and D. F. Hornig, J. Chem. Phys. 18, 1008 (1950).

2. S. B. Kormer, Sov. Phys. - Uspekhi 11, 229 (1968).

3. P. Harris and H.-N. Presles, J. Chem. Phys. 74, 6864 (1981).

4. P. Harris and H.-N. Presles, J. Chem. Phys. Jan 1984.

5. D. von der Linde in Ultrashort Light Pulses, S. L. Shapiro, ed. Vol 18 of Topics in Applied Phys. (Springer-Verlag, Berlin, 1977), a review article.

6. M. H. Rice and J. M. Walsh, J. Chem. Phys. 26, 824 (1957).

7. G. E. Walrafen, J. Chem. Phys. 40, 3249 (1964); 44, 1546 (1966).

8. J. E. Bertie and E. Whalley, J. Chem. Phys. 46, 1271 (1967).

9. P. Harris and H.-N. Presles, J. Chem. Phys. 77, 5157 (1982).

10. R. R. Alfano and S. L. Shapiro, Phys. Rev. Letters 26, 1247 (1971).

11. C. S. Coffey and E. T. Toton, J. Chem. Phys. 76, 949 (1982).

12. J. P. Kratohvil, M. Kerker, and L. E. Oppenheimer, J. Chem. Phys. 43, 914 (1965).

13. L. D. Landau and E. M. Lifshitz, Electrodynamics of Continuous Media (Addison-Wesley, Reading, 1960), section 93.

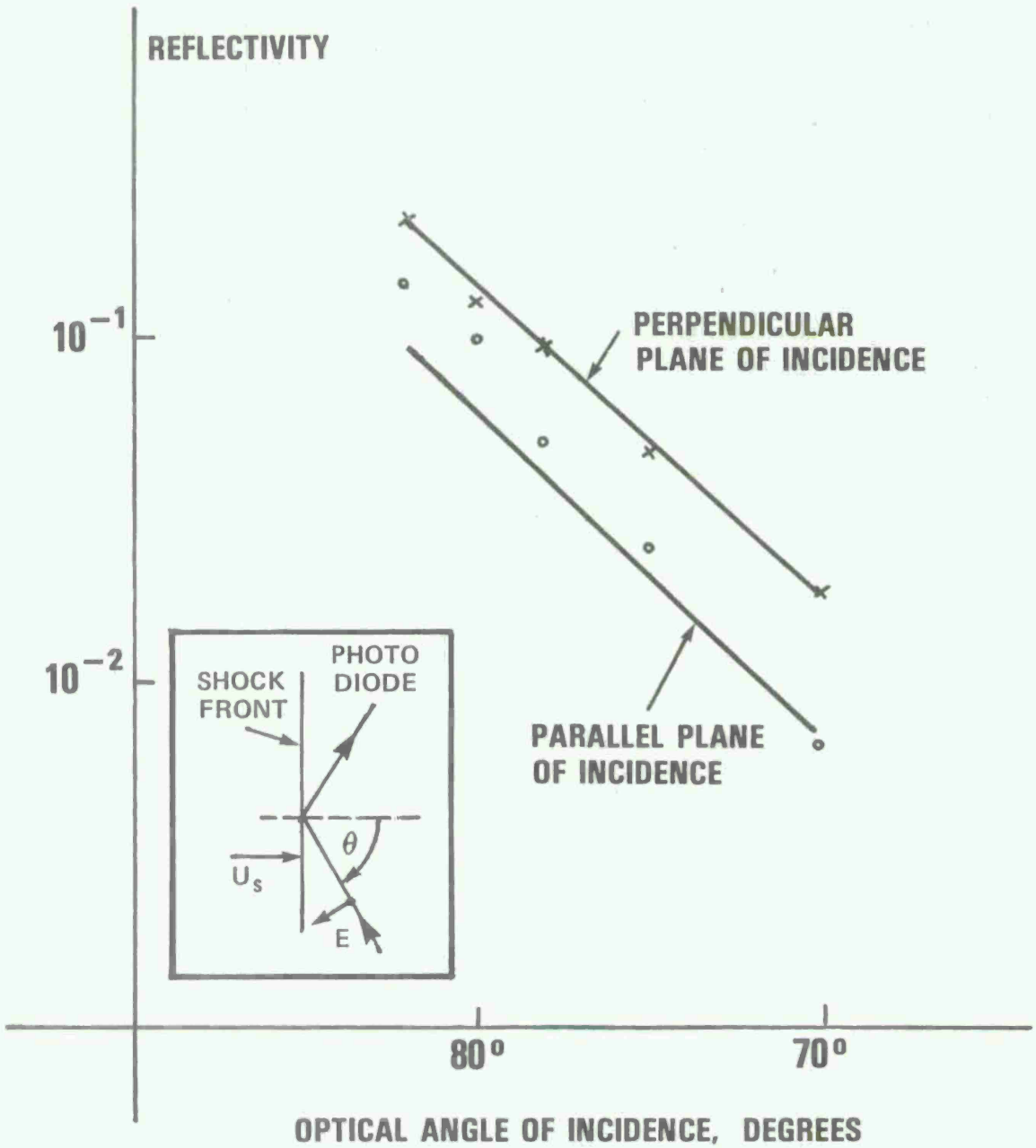

Theory for 5.8 kbar from reference 4. Insert shows reflectivity geometry for parallel-to-the-plane-of-incidence optical polarization. Reflectivity beam is a laser at 5145 Å (vacuum).

Figure 1. Water reflectivity data

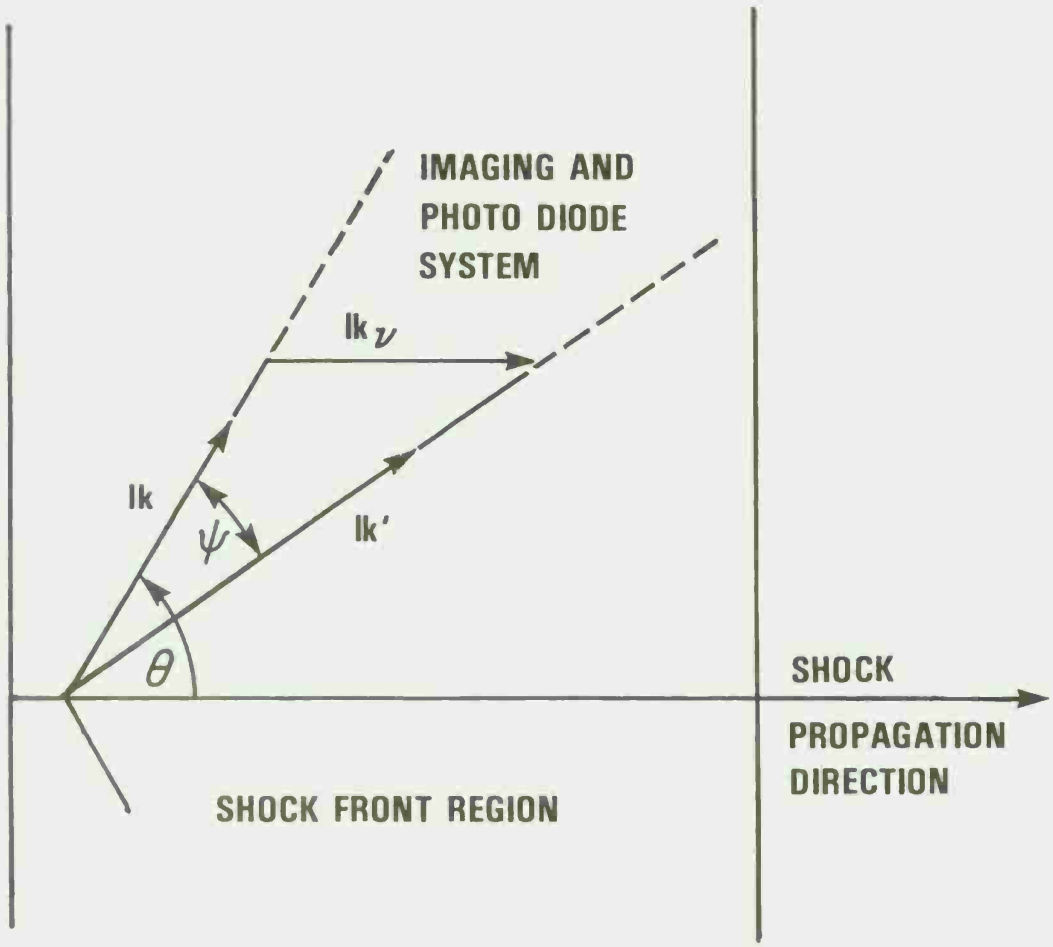

$\underset{\sim}{k}$ is the main reflectivity beam wave vector, $\underset{\sim}{k}'$ the sideband wave vector, and θ the optical angle of incidence.

Figure 2. Conservation of $\underset{\sim}{k}$ vector

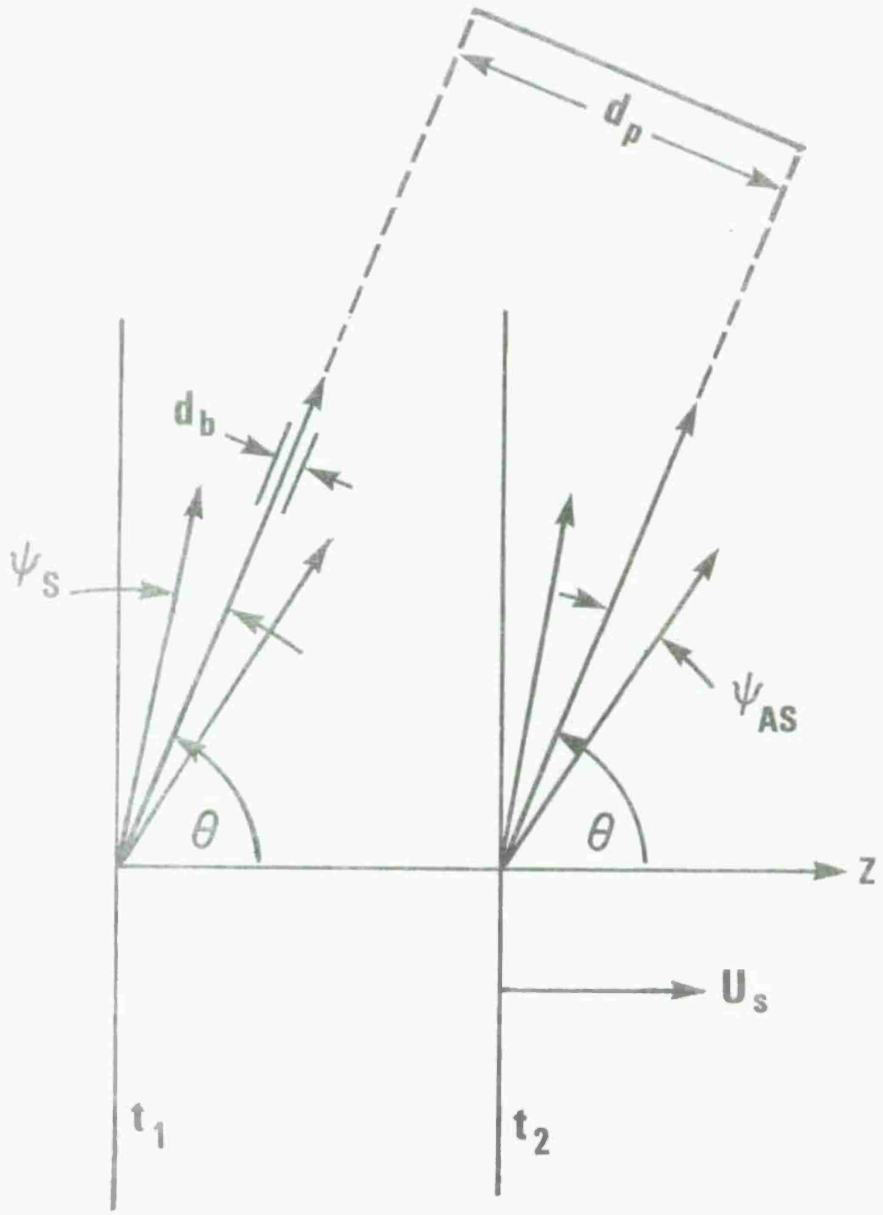

d_p is the photo-diode effective diameter, and t_1 and t_2 represent, respectively, the earliest and latest times for the main reflectivity beam to be imaged on the photo-diode (for vanishing beam diameter d_b). U_s is the shock velocity.

Figure 3. Photo-diode imaging geometry

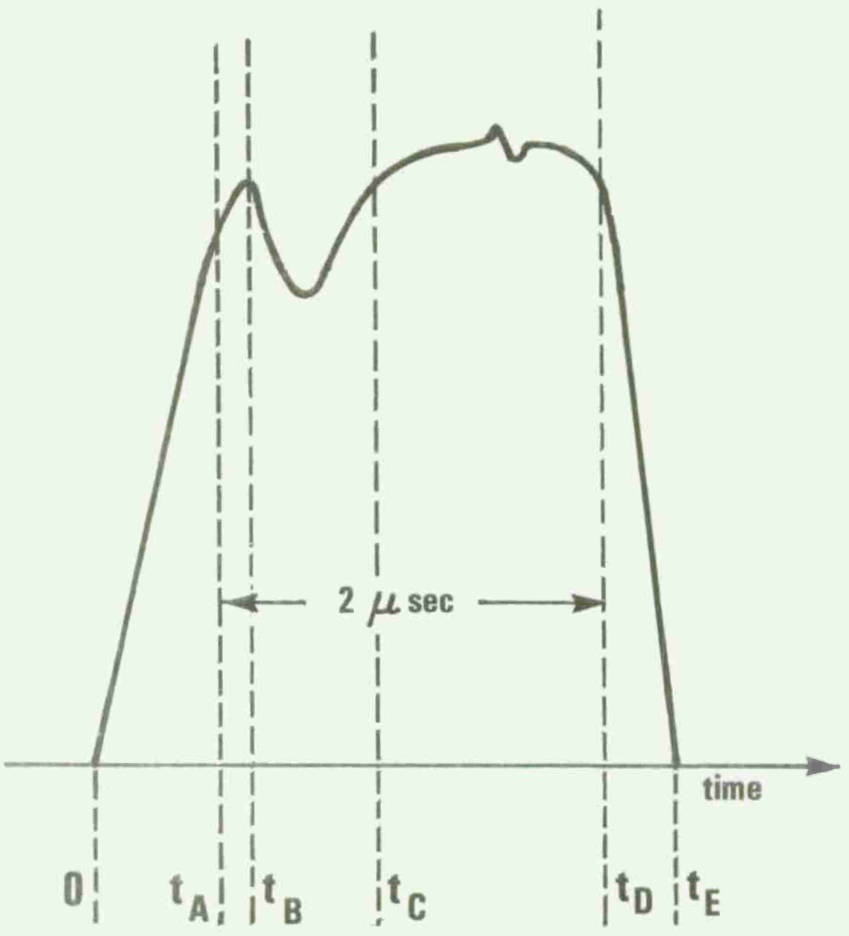

78 degree angle of incidence and parallel-to-the-plane-of-incidence optical polarization.

Figure 4. Noise averaged photo-diode record

DISTRIBUTION LIST

Commander
Armament Research and Development Center
U.S. Army Armament, Munitions
and Chemical Command
ATTN: DRSMC-TDC(D), D. Gyorog
DRSMC-TSS(D) (5)
DRSMC-LC(D), COL J. E. Brown
Deputy Director
DRSMC-LCN(D), H. Grundler
P. Harris (20)
T. Gora
W. Doremus
G. Vezzolli
DRSMC-LCE(D), R. Walker
Louis Avrami
F. Owens
C. Capellos
DRSMC-GCL(D)
Dover, NJ 07801

Director
Lawrence Livermore National Laboratory
ATTN: Frank E. Walker
A. M. Karo
W. J. Nellis
W. G. Von Holle
Livermore, CA 94550

Stanford Research Institute
Poulter Laboratories
ATTN: William J. Murri
D. R. Curran
R. K. Linde
Menlo Park, CA 94025

Sandia National Laboratory
ATTN: Walter Hermann
Robert Graham
D. B. Hayes
J. Gover
William Benedick
R. E. Hollenbach
L. D. Bertholf
P.O. Box 5800
Albuquerque, NM 87116

Washington State University
ATTN: George Duvall
G. R. Fowles
George Swan
Pullman, WA 99163

Commander
U.S. Naval Surface Weapons Center
Explosion Dynamics Division
ATTN: J. Sharma
C. S. Coffey
J. Forbes
James Goff
White Oak, MD 20910

Commander
U.S. Army Research Office
ATTN: J. Chandra
C. Boghosian
I. Lefkowitz
P.O. Box 12211
Research Triangle Park, NC 27709

Commander
U.S. Army Research and Standardization
Group (Europe)
P.O. Box 65
FPO 09510

National Bureau of Standards
ATTN: Donald Tsai
Henry Prask
Gaithersburg, MD 20760

California Institute of Technology
ATTN: Thomas J. Ahrens
Lien G. Yang
Pasadena, CA 91109

Department of Chemistry and
Chemical Engineering
ATTN: H. G. Drickamer
Urbana, IL 60436

Commander
Ballistics Research Laboratory
Armament Research and Development Center
U.S. Army Armament, Munitions
and Chemical Command
ATTN: DRSMC-BLT(A), Philip Howe
George E. Hauver

DRSMC-BLB(A), Donald Eccleshall
D. F. Strenzwilk
DRSMC-BLI(A), George Adams
I. May
DRSMC-BL(A), Robert F. Eichelberger
DRSMC-BLA-S(A)
Aberdeen Proving Ground, MD 21005

Chief
Benet Weapons Laboratory, LCWSL
Armament Research and Development Center
U.S. Army Armament, Munitions
and Chemical Command
ATTN: DRSMC-LCB-TL
Watervliet, NY 12189

University of Delaware
Department of Physics
ATTN: Ferd E. Williams
W. B. Daniels
Newark, DE 19711

Administrator
Defense Technical Information Center
ATTN: Accessions Division (12)
Cameron Station
Alexandria, VA 22314

Commander
U.S. Army Materials and
Mechanics Research Center
ATTN: John Mescall
D. P. Dandekar
Building 131
Arsenal Street
Watertown, MA 02172

Lockheed Palo Alto Research Labs
ATTN: J. F. Riley
3251 Hanover Street
Palo Alto, CA 94304

Bell Telephone Laboratories
ATTN: F. H. Stillinger
Murray Hill, NJ 07974

Director
Los Alamos Scientific Laboratory
ATTN: S. C. Schmidt
B. L. Holian
R. J. Trainov
D. C. Wallace
Los Alamos, NM 87544

Commander
U.S. Army Missile Command
ATTN: Charles M. Bowden
Redstone Arsenal, AL 35809

University of Tennessee
ATTN: M. A. Breazeale
Department of Physics and Astronomy
Knoxville, TN 37916

Princeton University
ATTN: A. C. Eringen
Princeton, NJ 08540

Carnegie Mellon Institute
of Technology
ATTN: Morton E. Gurtin
Bernard D. Coleman
Department of Mathematics
Pittsburgh, PA 15213

Brown University
ATTN: Robert T. Beyer
Department of Physics
Providence, RI 02912

Courant Institute of
Mathematical Sciences
ATTN: Library
New York University
New York, NY 10453

City College of the City
University of New York
ATTN: Harry Soodak
R. R. Alfano
Department of Physics
139th Street & Convent Ave
New York, NY 10031

Queens College of the City
University of New York
ATTN: Arthur Paskin
Department of Physics
Flushing, NY 11300

SPIRE Corporation
ATTN: Roger Little
Patriots Park
Redford, MA 01730

Director
U.S. Army Materiel Systems
Analysis Activity
ATTN: DRXSY-MP
Aberdeen Proving Ground, MD 21005

Commander
Chemical Research and Development Center
U.S. Army Armament, Munitions
and Chemical Command
ATTN: DRSMC-CLJ-L(A)
DRSMC-CLB-PA(A)
APG, Edgewood Area, MD 21010

Commander
U.S. Army Armament, Munitions
and Chemical Command
ATTN: DRSMC-LEP-L(R)
Rock Island, IL 61299

Director
U.S. Army TRADOC Systems
Analysis Activity
ATTN: ATAA-SL
White Sands Missile Range, NM 88002

Commander
Naval Research Laboratories
ATTN: E. F. Skelton
P. E. Schoen
E. S. Oran
Washington, DC 20375

UNCLASSIFIED

SECURITY CLASSIFICATION OF THIS PAGE *(When Data Entered)*

REPORT DOCUMENTATION PAGE		READ INSTRUCTIONS BEFORE COMPLETING FORM
1. REPORT NUMBER Technical Report ARLCD-TR-84002	2. GOVT ACCESSION NO.	3. RECIPIENT'S CATALOG NUMBER
4. TITLE *(and Subtitle)* SHOCK FRONT PUMPED STOKES AND ANTI-STOKES REFLECTIVITY CONTRIBUTIONS		5. TYPE OF REPORT & PERIOD COVERED FY84 6. PERFORMING ORG. REPORT NUMBER
7. AUTHOR(s) Paul Harris, ARDC Henri-Nöel Presles, University Poitiers, France		8. CONTRACT OR GRANT NUMBER(s)
9. PERFORMING ORGANIZATION NAME AND ADDRESS ARDC, LCWSL Nuclear and Fuze Div [DRSMC-LCN(D)] Dover, NJ 07801		10. PROGRAM ELEMENT, PROJECT, TASK AREA & WORK UNIT NUMBERS Project 1L161102AH60
11. CONTROLLING OFFICE NAME AND ADDRESS ARDC, TSD STINFO Div [DRSMC-TSS(D)] Dover, NJ 07801		12. REPORT DATE March 1984 13. NUMBER OF PAGES 25
14. MONITORING AGENCY NAME & ADDRESS *(if different from Controlling Office)*		15. SECURITY CLASS. *(of this report)* UNCLASSIFIED 15a. DECLASSIFICATION/DOWNGRADING SCHEDULE

16. DISTRIBUTION STATEMENT *(of this Report)*

Approved for public release; distribution unlimited.

17. DISTRIBUTION STATEMENT *(of the abstract entered in Block 20, if different from Report)*

18. SUPPLEMENTARY NOTES

19. KEY WORDS *(Continue on reverse side if necessary and identify by block number)*

Shock waves
Shock front
Shock structure
Shock front optical reflectivity

20. ABSTRACT *(Continue on reverse side if necessary and identify by block number)*

It is claimed that mass density shock pumped excited states can be converted to Stokes and Anti-Stokes radiation which would contribute to shock front optical reflectivity signals in liquid water at 5.8 kbar. The experimental status and relevant theory are described in detail.

DD FORM 1 JAN 73 1473 EDITION OF 1 NOV 65 IS OBSOLETE

SECURITY CLASSIFICATION OF THIS PAGE *(When Data Entered)*